

Imaging human reward processing with positron emission tomography and functional magnetic resonance imaging

Nina B. L. Urban · Mark Slifstein · Shashwath Meda · Xiaoyan Xu · Rawad Ayoub ·
Olga Medina · Godfrey D. Pearlson · John H. Krystal · Anissa Abi-Dargham

Received: 17 June 2011 / Accepted: 11 October 2011
© Springer-Verlag 2011

Abstract Functional neuroimaging (fMRI) studies show activation in mesolimbic circuitry in tasks involving reward processing, like the Monetary Incentive Delay Task (MIDT). In voltammetry studies in animals, mesolimbic dopamine release is associated with reward salience. This study examined the relationship between fMRI activation and magnitude of dopamine release measured with Positron

emission tomography study (PET) in the same subjects using MIDT in both modalities to test if fMRI activation is related to dopamine release. Eighteen healthy subjects were scanned with [¹¹C]raclopride PET at baseline and after MIDT. Binding potential (BP_{ND}) was derived by equilibrium analysis in striatal subregions and percent change across conditions (Δ BP_{ND}) was measured. Blood oxygen level dependence (BOLD) signal changes with MIDT were measured during fMRI using voxelwise analysis and ROI analysis and correlated with Δ BP_{ND}. Δ BP_{ND} was not significant in the ventral striatum (VST) but reached significance in the posterior caudate. The fMRI BOLD activation was highest in VST. No significant associations between Δ BP_{ND} and change in fMRI BOLD were observed with VST using ROI analysis. Voxelwise analysis showed positive correlation between BOLD activation in anticipation of the highest reward and Δ BP_{ND} in VST and precommissural putamen. Our study indicates that endogenous dopamine release in VST is of small magnitude and is related to BOLD signal change during performance of the MIDT in only a few voxels when rewarding and nonrewarding conditions are interspersed. The lack of correlation at the ROI level may be due to the small magnitude of release or to the particular dependence of BOLD on glutamatergic signaling.

N. B. L. Urban · M. Slifstein · X. Xu · R. Ayoub · O. Medina ·
A. Abi-Dargham
Department of Psychiatry at Columbia University,
New York, NY, USA

S. Meda
Center for Human Genetics and Research, Vanderbilt University,
Nashville, TN 37232, USA

M. Slifstein · A. Abi-Dargham
Radiology at Columbia University,
New York, NY, USA

M. Slifstein · A. Abi-Dargham
New York State Psychiatric Institute,
New York, NY, USA

G. D. Pearlson · J. H. Krystal
Department of Psychiatry at Yale University,
New Haven, CO, USA

G. D. Pearlson
Olin Neuropsychiatry Research Center, Institute of Living,
Hartford, CT, USA

J. H. Krystal
VA Alcohol Research Center, VA Connecticut Healthcare System,
West Haven, CT, USA

N. B. L. Urban (✉)
NYSPI, Department of Psychiatry,
1051 Riverside Dr., Unit 31,
New York, NY 10032, USA
e-mail: nu2118@columbia.edu

Keywords Human reward processing · Dopamine · MIDT ·
PET · fMRI

Introduction

Dopamine (DA) is closely associated with reward-seeking behaviors including approach, consumption, and addiction (Arias-Carrion and Poppel 2007). Reward processing in the central nervous system depends largely on the activity of DA-releasing neurons located within the ventromedial

substantia nigra (pars compacta, SNc) and ventral tegmental area (VTA). Electrophysiological studies in nonhuman primates show increased firing rate, predicting increased DA release in terminal regions, in response to unpredictable rewards, while no response is elicited from fully predictable rewards ('reward consumption'), and prolonged activation seen with delayed rewards ('anticipation'). Depression of firing is observed when expected rewards are omitted ('punishment') (Schultz et al. 1992; Schultz 1998).

These findings led to the "reward prediction error hypothesis" (Bayer and Glimcher 2005): DA neurons respond to the difference between how rewarding an event is experienced vs. the anticipated reward—a signal used to update the value attached to different actions and the main basis for the assumption that DA is involved in reinforcement learning (Sutton and Barto 1998), driving behavior.

The nucleus accumbens (NAcc) in the VST is a major target of midbrain DA projections especially those arising in the VTA. Human functional neuroimaging (fMRI) studies found activation of the SNc/VTA and the VST during reward anticipation (Knutson et al. 2000; Knutson et al. 2001a, b). When monetary gains and losses were used as incentives, VTA BOLD responses were thought to reflect positive reward prediction errors modulated by the probability of winning (D'Ardenne et al. 2008). The anticipation phase revealed proportional activation for increasing levels of reward, suggesting that motivation for goal-directed behavior largely depended on the expected value of the anticipated reward (Rademacher et al. 2010).

Studies examining the role of striatal DA and reward learning in humans demonstrated that individual differences in reward-related learning reflect variation in baseline striatal DA synthesis capacity as measured with uptake of [¹⁸F]fluorometatyrosine (Cools et al. 2009). Also, heterozygote carriers of a specific polymorphism in the untranslated region of the DA transporter gene (DAT1), associated with high striatal DA, showed greater activity in the VST during reward anticipation than homozygotes as well as greater activity in the dorsomedial striatum during anticipation of high reward vs. low reward (Aarts et al. 2010).

Reward sensitivity-based paradigms such as the Monetary Incentive Delay Task (MIDT) activate a "reward circuit" that includes the NAcc, amygdala, midbrain, VTA, mesial prefrontal cortex, caudate, putamen, hippocampus, anterior cingulate, insula and orbitofrontal cortex (OFC) (Knutson et al. 2005). The contribution of DA signaling to the fMRI BOLD signal detected during rewarding tasks has not been extensively studied. Initial Positron emission tomography study (PET) studies have explored behavioral effects on D2/3 receptor antagonist radiotracer binding. Koeppe et al. found PET [¹¹C]raclopride binding was significantly reduced after a goal-directed motor task compared to baseline consistent with competition from task induced DA release (Laruelle 2000).

The reduction in binding potential correlated positively with the performance level during the task and was greatest in the VST (Koeppe et al. 1998). Additionally, rewarded tasks were associated with a stronger striatal [¹¹C]raclopride BP_{ND} decrease than nonrewarded tasks with comparable sensorimotor activity (Zald et al. 2004), and a positive correlation was found between neural activity of the SNc/VTA during reward anticipation (evaluated with fMRI and a modified MIDT) and reward-related [¹¹C]raclopride displacement in VST in the same subjects (Schott et al. 2008).

Here, we present a study with PET and fMRI aimed at assessing reward-related DA release and BOLD activation in the same subjects in response to a modified MIDT (Knutson et al. 2000). We hypothesized that MIDT induces DA release detectable as decrease in binding potential (BP_{ND}) of the D2/3 radiotracer [¹¹C]raclopride compared to baseline and that percent decrease (Δ BP_{ND}) would correlate with fMRI BOLD activation in the corresponding regions.

Material and methods

Study population

Eighteen to 45 years old, medically and psychiatrically healthy male and female volunteers of all ethnicities participated in study as shown in Table 1. Exclusion criteria were pregnancy or lactation for women, current use of psychotropic medication, presence or positive history of severe medical illness and history of prior or current substance abuse or dependence. Offspring of alcoholic mothers were excluded to avoid alcohol fetopathy. Eligibility criteria were ascertained with the Structured Clinical Interview for DSM-IV (SCID, (First et al. 1995)), physical exam, and basic clinical screening tools (electrocardiogram, comprehensive laboratory tests and urine toxicology).

Study design

The study consisted of two [¹¹C]raclopride PET scans performed on the same day and one fMRI scan performed

Table 1 Demographics. Shown are demographics for all subjects who completed PET scans and the subgroup that also completed fMRI with the MIDT

Demographics	PET	fMRI
N	18	15
Age (years)	29.1±6.4	28.6±5.5
Gender	9 M, 9 F	8 M, 7 F
Smokers	0	0
Ethnicity (C,AA,H,As)	4,9,3,2	3,8,2,2

within 1 month of PET in a counterbalanced order (eight subjects received fMRI first, ten subjects PET scans first). MIDT was performed during each imaging modality.

Monetary Incentive Delay Task (MIDT)

The MIDT was modified from a design published by Knutson (Knutson et al. 2000) as described in Andrews et al. (2010). The same paradigm was used for both PET and fMRI studies. Subjects engaged in one 24-minute session of the MIDT before the PET scan and two 12-minute sessions during fMRI scan acquisition. Sessions consisted of 55 13-second trials. Trials were contiguous and included a cue, an anticipation phase, the response to a target, and feedback. During each incentive trial, participants saw one of six word cues (“WIN \$ 0/1/5”. “LOSE \$0/1/5”, duration=1,000 ms) followed by a fixation on a crosshair (anticipatory interval 1, A1, “prospect of reward”) before responding with a button press (one of two depending on the cue “win” or “lose”) to the target in the form of a white rectangle. During the anticipatory interval 2 (A2, “anticipation of reward”), subjects fixated on a crosshair again before finally receiving feedback notifying them if they had won or not (outcome of reward) or lost or avoided loss (outcome of loss) of money during that trial as well as of their cumulative winnings. The ‘outcome’ represented the consummatory phase (Fig. 1). Sufficiently fast responses resulted in rewards/nonlosses, slow or incorrect responses in nonrewards. Task difficulty, modified by three possible time durations for the target, was individually calibrated according to reaction times (RT) collected during a 5-minute prescan practice session. During fMRI, volume acquisitions were time-locked to the offset of each cue and thus acquired during anticipatory delay periods. Compared to the original task, a neutral stimulus of Win/lose \$0 was added, the timing of all viewing conditions (A1, A2 and outcome of reward and loss) were extended to more clearly separate them, the “reward anticipation”, “A2” period was modeled separately from the outcome period and fixed event onset was added to minimize intercorrelations across regions in order to better separate different periods in the fMRI analysis. Our modified version also incorporated an

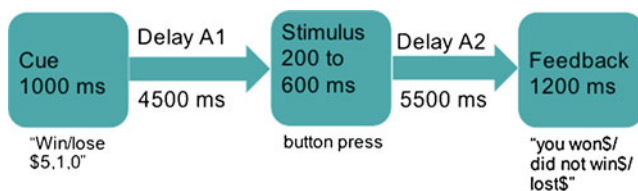


Fig. 1 Monetary Incentive Delay Task (MIDT). Represented is one trial in the MIDT, including cue, prospect of reward/punishment (A1), stimulus (box), anticipation of reward/punishment (A2), and feedback (outcome, OC) with respective durations

adjusted win: negative outcome ratio of 64:36 to make the task more salient by keeping a favorable win ratio. Subjects received payment of the amount earned during the task, a maximum of \$138 on the PET day and \$132 during fMRI. Subjects were asked a series of postscan debriefing questions to assess their subjective response to each condition of the task (Subjective Experience Rating Scale, SER), rated on a scale from 1 (very unhappy) to 5 (very happy).

Positron emission tomography study (PET)

PET data acquisition

PET scans were conducted at Milstein Hospital, Columbia University Medical Center on an ECAT EXACT HR+ scanner (Siemens Medical Systems, Knoxville, TN, USA). Subject preparation included placement of two venous catheters, one for radiotracer infusion and one for blood sampling and a blood pregnancy test. Reduction of head movement was achieved with a polyurethane head immobilizer system molded around the head of the subject. Baseline scans preceded scan with MIDT.

For each of the two scans, [^{11}C]raclopride was administered as a bolus plus constant infusion (3-minute bolus, 80-minute infusion, total injected volume=60 mL) (Mawlawi et al. 2001; Martinez et al. 2003). The decay corrected radioactivity was limited to 15 mCi at the time of the bolus and the [^{11}C]raclopride mass dose did not exceed 6.54 μg . Subjects were positioned in the PET scanner 25 min into the infusion. Emission data were collected in the 3D mode for 40 min, obtained from 40 to 80 min after the bolus, as eight successive frames of 5-minute duration. A 10-minute transmission scan was obtained at the end of the emission scans. Venous blood samples were drawn manually at 40, 50, 60, 70 and 80 min to measure tracer concentration and free fraction (f_p) in plasma and for calculation of the distribution volume of [^{11}C]raclopride in the cerebellum (V_{ND}).

MIDT was started 5 min before the second [^{11}C]raclopride injection and continued for 24 min while the subject was seated outside of the PET scanner (Fig. 2).

PET data analysis

Image analysis was performed as described previously (Mawlawi et al. 2001). PET data were coregistered to individual subjects' structural MRI scans obtained prior to fMRI, using maximization of mutual information as implemented in SPM2 (Ashburner 2009). Regions of interest (ROIs) were drawn on each individual's MR image and applied to the coregistered PET images. The striatum was divided into five anatomical ROIs including pre- and postcommissural putamen (preDPU, postPU), pre- and

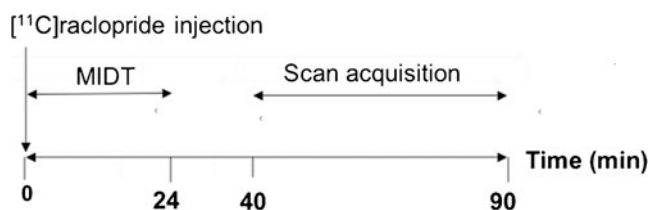


Fig. 2 Timeline of PET scan. Schematic representation of administration of Monetary Incentive Delay Task during PET. Beginning of MIDT coincided with the [¹¹C]raclopride bolus injection and was carried out outside of the PET scanner for 24 min. The subject was then placed inside the camera and emission scan started 40 min after initial tracer injection

postcommissural caudate (preDCA, postCA) and VST as described previously (Martinez et al. 2003). Functional subdivisions analyzed separately consisted of the associative striatum (AST=preDPU+preDCA+postCA), sensorimotor striatum (SMST=postPU), VST and striatum as a whole (sum of all anatomical ROI) (Haber et al. 2000). Cerebellum (CER) was used as a low D2/3 receptor reference region to measure free and nonspecifically bound [¹¹C]raclopride activity (Hall et al. 1994). Equilibrium analysis was used to derive the specific to nondisplaceable equilibrium partition coefficient BP_{ND} (unitless) as ROI activity/CER activity-1 during steady state (Martinez et al. 2005). The distribution volume of nondisplaceable [¹¹C]raclopride (V_{ND}) was computed as the ratio of cerebellum activity to unmetabolized [¹¹C]raclopride in venous plasma at equilibrium. Steady state conditions were verified by calculating the slopes of ROI activity over 40 min (Laruelle et al. 1994; Martinez et al. 2003).

The primary outcome measure for the study was the percent change in BP_{ND} between conditions (ΔBP_{ND}), calculated as:

$$\Delta BP_{ND} = [(BP_{NDMIDT}/BP_{NDbaseline}) - 1] \times 100\%,$$

expressing the relative reduction in D2/3 receptor availability for [¹¹C]raclopride binding after MIDT induced DA release.

Statistical analysis

Comparisons between baseline and postMIDT were performed with paired *t*-tests. A two-tailed probability value of $p < 0.05$ was chosen as statistically significant.

Functional MRI study

Image acquisition

Functional data were acquired on a 3 T GE Sigma MR scanner (GE Healthcare, Waukesha, Wisconsin) at the

New York State Psychiatric Institute, Columbia University Medical Center, using an echoplanar sequence (TR=1,500 ms, TE=27 ms, FOV=22 cm, flip angle=70°, acquisition matrix=64×64, voxel size=3.44×3.44, slice thickness=5 mm, number of slices=29, acquired in a sequential order). The subjects used an MRI-compatible hand-held response pad for responding to the task (multibutton response unit). The MIDT task was viewed through dual channel binocular goggles. For the purpose of anatomical coregistration of PET, a T1-weighted structural MRI was acquired for each subject prior to fMRI.

Data processing and analysis

fMRI data

Analyses focused on changes in activation specifically during anticipatory delay periods for both hit and miss trials (i.e., after subjects saw cues but before they responded to targets) as described in Andrews et al. (2010). Task phases were compared to the relevant neutral conditions Win/lose \$0, Win\$0, and lose\$0 as well as to the implicit baseline. Functional images were preprocessed using SPM2 (Wellcome Department of Imaging Neuroscience, UCL, UK, (Ashburner 2009), running in Matlab 7.1 (Mathworks, Natick, MA) on a Linux platform. The first six images of each time series were removed to compensate for saturation effects. Data were motion-corrected using INRIAAlign and then spatially normalized to the standardized EPI template image in SPM2. After normalization, images were spatially smoothed with a 9-mm isotropic kernel.

Statistical comparisons

For each subject, regressors were formed by convolving impulses at the times of events with a hemodynamic response function. Subjects' data were fitted to a linear sum of these responses, generating coefficients (β s) for the BOLD response to each condition during the trial at each voxel (β maps). Group level analyses were then applied to the β maps with contrasts for prospect of \$5 reward (A1), the maximal reward, or anticipation of \$5 reward (A2) vs. all neutral conditions (Win or lose \$0, implicit baseline). We also evaluated the same set of contrasts for \$1 win and \$5 and \$1 losses. Statistical maps (voxel by voxel *t*-statistics) were created in SPM2 and analyzed with small volume correction for multiple comparisons using a mask of the VST as defined in the PET ROI analysis. The anatomical location and the spatial validity of the VST mask were verified independently by three imaging analysts (S.M., G.P. and X.X.). Corrections for multiple compar-

isions were performed using the false discovery rate criterion (FDR) with $p=0.05$ as the corrected significance level.

Correlational analysis of fMRI and PET data

As the primary aim of our study was the identification of BOLD indices of endogenously released DA, fMRI contrasts were compared with [^{11}C]raclopride $\Delta\text{BP}_{\text{ND}}$. Two sets of analyses were performed. In the first, voxel-based analysis, fMRI contrasts between rewarded conditions and both implicit baseline and “Win/lose\$0” were tested for correlation (Pearson product moment coefficient) with regional $\Delta\text{BP}_{\text{ND}}$ (for each ROI). “Implicit baseline” refers to the activation left after all effects from contrasts have been removed. In a second, ROI-based analysis, an ROI average was computed from each subject's β differences (for each contrast of interest) in each ROI and tested for correlation with PET $\Delta\text{BP}_{\text{ND}}$ from the same region. A probability value of $p<0.05$ was chosen as statistically significant.

Results

Subjects

Eighteen subjects completed both PET and fMRI scans. FMRI data from three subjects had to be excluded from analysis due to technical problems with the scan data (partial recording). See Table 1 for demographics.

Behavioral data

Subjects reliably recognized cues during the task in both imaging modalities. The average time to respond (RT) to each trial condition (Win/lose\$5, Win/lose\$1, Win/lose\$0) did not differ significantly between trials nor between fMRI and PET, although there was a trend to slower RT during the PET task (fMRI: 209.5 ± 22.2 ms, PET: 237.4 ± 56.0 ms; $p=0.07$). A paired t -test revealed no significant differences between the two performances of the task within subject ($p=0.17$).

The average total monetary reward for the fMRI task was $\$77.3\pm \21.8 and for PET $\$86.1\pm \35.2 ($p=0.44$). There was no significant correlation between fMRI activation or [^{11}C]raclopride displacement in any region and individual monetary rewards.

Participants rated the experience with higher mean scores for the more rewarding trials on SER (“Won/did not lose\$5”: 4.4 ± 0.6), lower scores for the least rewarding/most punishing trials (“Lost/did not win\$5”: 1.4 ± 0.6), and intermediate scores for the neutral trials in both imaging modalities (“Won/did not lose\$0: 2.7 ± 0.7).

Imaging results

Effect of MIDT on DA release (PET)

Table 2 shows scan parameters for all subjects. There were no significant differences between conditions in any of these. There was a small, average overshoot of steady state that was not significantly different between conditions (activity decrease in the whole striatum: $11.0\pm 11\%$ per hour at baseline, $10.5\pm 11.8\%$ per hour after MIDT, $p=0.819$, paired t -test).

For right and left sides combined, $\Delta\text{BP}_{\text{ND}}$ between baseline and MIDT was only significantly different in the postCA ($\Delta\text{BP}_{\text{ND}}=-6.4\pm 10.1\%$, $p=0.009$) that survived Bonferroni correction for multiple comparisons across $n=5$ subregions ($p=0.047$). Baseline BP_{ND} and $\Delta\text{BP}_{\text{ND}}$ in all ROIs are displayed in Table 3. When separating right and left sides for all ROIs, displacement was significantly different from 0 in postCA both on the right and on the left ($-5.6\%\pm 10.3\%$, $p=0.03$; $-7.0\%\pm 12.9\%$, $p=0.02$, respectively) and in AST on the left ($-3.7\%\pm 6.8\%$, $p=0.03$). Magnitude of $\Delta\text{BP}_{\text{ND}}$ was numerically greater on the left side but the difference between sides did not reach statistical significance.

There were no significant correlations between BP_{ND} and RT in any ROI for either PET or fMRI.

fMRI data of reward anticipation

Rewarded trials were compared with control trials of both the rewarded and the neutral condition (weighted 1:3, proportionally to the total number of cues). In line with previous studies, reward anticipation was associated with activation of numerous mesolimbic regions involved in the reward network. Compared with neutral cues, reward-predicting cues were associated with an increased fMRI response in the VST and caudate.

Table 2 Scan parameters. Injected dose (ID), injected mass (IM), specific activity (SA), distribution volume of the reference region (V_{ND}) plasma-free fraction (f_{p}) and brain-free fraction (f_{ND}) are shown. Parameters did not differ between conditions or groups

PET parameters	PET ($n=18$)		
	Baseline	MIDT	paired t (p)
ID (mCi)	8.38 ± 1.39	8.26 ± 1.45	0.83
IM (μg)	3.65 ± 1.22	4.07 ± 1.69	0.22
SA (Ci/mmol)	$1,374\pm 594$	$1,317\pm 738$	0.68
V_{ND}	0.50 ± 0.15	0.49 ± 0.12	0.91
f_{p}	$4.03\pm 0.57\%$	$4.00\pm 0.62\%$	0.86
f_{ND} ($f_{\text{p}}/V_{\text{ND}}$)	$8.57\pm 2.10\%$	$8.54\pm 2.22\%$	0.94

Table 3 Bilateral binding potential. [^{11}C]raclopride binding (BP_{ND}) for all regions of interest (ROI), right and left sides combined, at baseline and after MIDT. $\Delta\text{BP}_{\text{ND}}$ is the percent difference between conditions. Significant differences in binding were found in the posterior caudate (postCA)

ROI	Baseline (BP_{ND})	MIDT (BP_{ND})	$\Delta\text{BP}_{\text{ND}}$	<i>p</i>
VST	2.15±0.24	2.13±0.32	-1.0±9.7%	0.65
AST	2.53±0.27	2.45±0.35	-3.2±6.9%	0.07
PreDCA	2.50±0.29	2.42±0.40	-3.5±8.9%	0.12
PreDPU	2.83±0.29	2.77±0.33	-2.0±6.9%	0.23
PostCA	1.99±0.31	1.87±0.39	-6.4±10.1%	<i>0.01</i>
PostPU	3.05±0.36	3.00±0.41	-1.9±7.1%	0.27
STR	2.64±0.27	2.57±0.35	-2.7±6.6%	0.12

Statistically significant p-values appears in italics

fMRI activation

Consistent with previous studies using similar versions of the MIDT, the most robust activation was detected for the contrast A1 Win \$5–A1 Lose \$0, and showed activation in VST ($T=5.45$, FDR-corrected $p=0.062$, peak voxel coordinates $[x, y, z]=[24, 18, -9]$) and caudate nucleus ($T=5.41$, FDR-corrected $p=0.062$, peak voxel coordinates $[21, 18, 6]$); however, only reaching trend level significance. The local maximum for activation in the anterior cingulate was located at $[12, 9, 42]$ ($T=4.55$, FDR-corrected 0.082). SPM results ($n=15$) for “A1Win \$5–A1 Lose \$0”, T map display threshold: $p=0.001$ uncorrected, are shown in (Fig. 3). Using “Win/lose\$0” combined as a baseline contrast showed weaker activation, contrast with Win\$0 alone showed no activation in key regions of the reward circuit. As expected, no significant effects were observed for contrasts of neutral conditions (Win/lose\$0 A1 vs. implicit baseline). Activation peaks coincided with the anticipatory delay and anticipatory activation did not differ as a function of outcome. None of the contrasts for A2 (“A2Win \$5–A2 Lose or A2Win\$0 or A2Win/lose\$0”) showed significant activation.

Correlations of fMRI activation with $\Delta\text{BP}_{\text{ND}}$

The volumes of ROIs drawn on MR images in MNI space were 5,088 mm³ for postCA, 4,760 mm³ for preDPU, 2,240 mm³ for VST, 904 mm³ for preDCA, and 4,544 mm³ for postPU with a volume of $2 \times 2 \times 2$ mm³ per voxel. In the first, voxel-based analysis, fMRI contrasts between rewarded conditions and implicit baseline were tested for correlation with regional $\Delta\text{BP}_{\text{ND}}$ (for each ROI). Voxelwise correlation analysis between contrast values and $\Delta\text{BP}_{\text{ND}}$ showed positive correlation between the A1 Win \$5 vs. baseline contrast and ($-\Delta\text{BP}_{\text{ND}}$) in the preDPU ($T=5.45$, FDR-corrected p -value=0.03, peak voxel MNI coordinates

$[x, y, z]=[21, 9, -6]$). These coordinates were located in the VST (Fig. 4). The contrast between “outcome of all wins” and baseline also correlated at trend level with $\Delta\text{BP}_{\text{ND}}$ in VST ($T=5.45$, FDR-corrected p -value=0.062, peak voxel coordinates $[x, y, z]=[-15, 9, 12]$). Table 4 shows significant correlations between $\Delta\text{BP}_{\text{ND}}$ in other ROI and their localization. Table 5 shows correlations between ROI averages of fMRI contrasts (% change in BOLD signal as well as β coefficients) and $\Delta\text{BP}_{\text{ND}}$ in the VST and postCA for the contrasts of largest activation (Win/lose\$5 vs. Win/lose\$0). The correlation reached a level of statistical significance for several contrasts (not displayed), but none survived correction for multiple comparison.

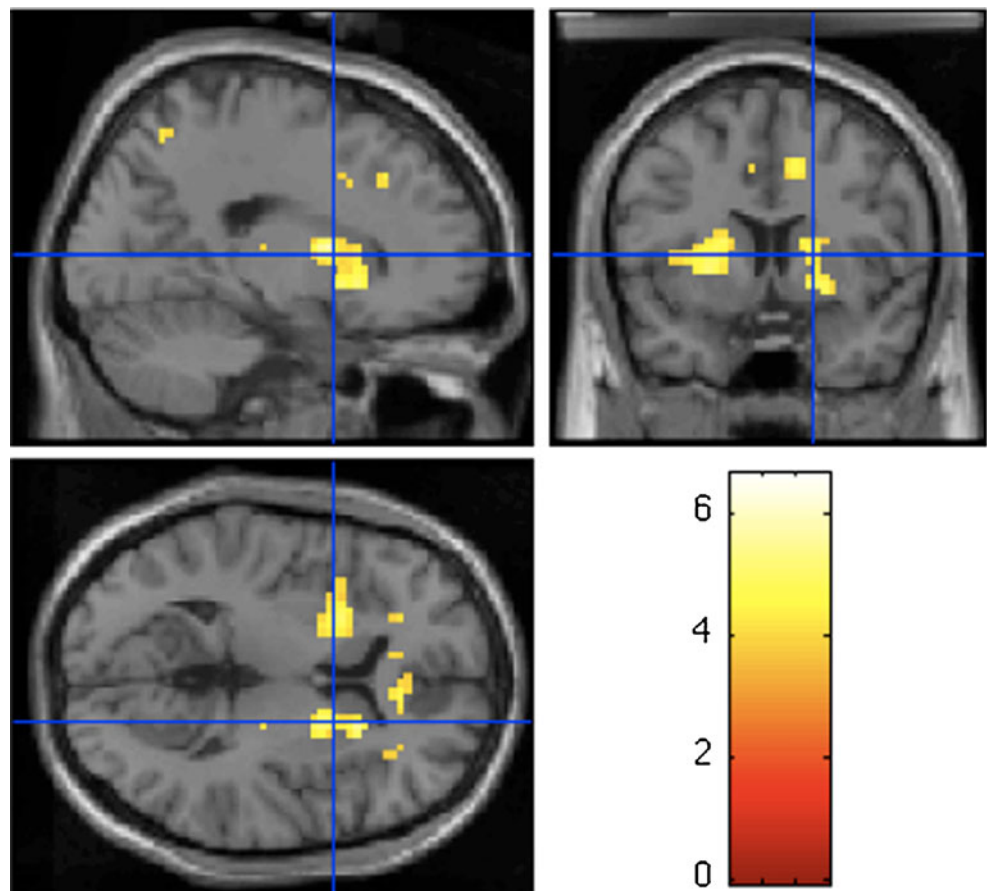
Discussion

We evaluated MIDT-induced DA release in striatal regions with PET and MIDT-induced BOLD activation with fMRI in the same subjects. We examined DA release induced by all phases and trials of the task combined together for PET, while we examined activation to different phases and conditions of the task with fMRI: A1 as the prospect of reward indicated by a cue, A2 equaling anticipation of reward after response to the cue, and OC, consummation of reward. We failed to detect a change in [^{11}C]raclopride binding in the primary area of reward processing (VST) but detected a significant change in the postCA. With fMRI, we observed the typical pattern of activation in regions involved in reward-processing, although they did not reach statistical significance. Voxelwise analysis found significant correlations for fMRI contrasts between the highest reward condition vs. implicit baseline and regional $\Delta\text{BP}_{\text{ND}}$ localizing to the VST, but we failed to detect a relationship between the two imaging modalities' outcome measures in the ROI-based analysis of correlations between $\Delta\text{BP}_{\text{ND}}$ and subjects' β coefficients in the corresponding ROI. Our study is consistent in some respects with previous findings comparing DA release in a rewarded task with the hemodynamic reward anticipation response to the same task in young healthy adults (Schott et al. 2008) and provides further evidence to understand physiological correlates of fMRI activation in human reward circuitry.

fMRI

In our hands, the fMRI MIDT paradigm produced a similar pattern of activation in reward-processing regions as in previous studies, with the strongest signal in response to the most rewarding trial anticipation found in the VST. We observed activation in similar regions as previously reported (Knutson et al. 2000; Knutson et al. 2001a, b; Schott et al. 2008; Andrews et al. 2010), with activated

Fig. 3 *t*-Statistics map for contrast “A1Win\$5 vs. A1Lose \$0” ($n=15$); the voxels of greatest intensity had the coordinates $[x, y, z]=[24, 18, -9]$ ($T=5.45$, $FDR p=0.062$), and $[21, 18, 6]$ ($T=5.41$, $FDR p=0.062$). This corresponded to the VST and the caudate nucleus, respectively. The crosshairs are located at $[18, 8, 5]$ in the caudate. The slice shown was chosen in order to depict both activation maxima. As per radiological convention, left is on the right and vice versa



areas in caudate, putamen, mesial prefrontal cortex/anterior cingulate, and left motor cortex. Schott et al. found that “punishment” trials also revealed additional activation in thalamus and anterior cingulate. While we also found activation in these areas for the most rewarding contrasts, punishment trials showed a more diffuse pattern.

Similar to Schott et al. (2008), stimuli only elicited activation when paired with incentive value in our study; we found no discernible pattern in the fMRI statistical maps for

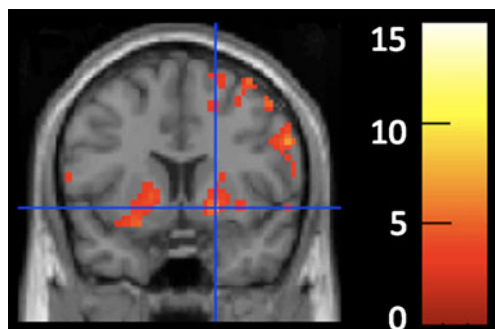


Fig. 4 Coronal view of *t*-statistics map for “A1W\$5 vs. implicit baseline” correlated with ΔBP_{ND} in the preDPU ($n=15$); $FDR=0.03$ at the peak coordinates $[x, y, z]=[21, 9, -6]$, which were located in the VST (indicated by the *crosshair*). As per radiological convention, left is on the right and vice versa

neutral contrasts (W\$0/L\$0 vs. baseline). This also reduces the likelihood that activation merely reflected motor responses as the observed patterns were specific to incentive trials.

We found greater activation in VST for the anticipatory phase A1 than the consummatory phase OC. A1 is the phase best described as the opportunity—vs. expectation or consumption—of reward. This is consistent with the finding that VTA DA neurons fire more readily to cues that predict potential reward than to reward delivery per se in animal studies (Schultz et al. 1997).

Peak fMRI activation in response to the highest reward condition was in the VST or closely associated areas. We

Table 4 Voxel-based analysis for Pearson product moment correlations between fMRI contrasts and regional ΔBP_{ND} . Shown are ROI for which ΔBP_{ND} was significantly correlated with the fMRI contrast for A1Win\$5 vs. implicit baseline, the locus of the correlated voxel, *T* values, *FDR*-corrected *p*-values and the peak voxel coordinates according to the Montreal Neurological Institute (MNI)

ΔBP_{ND} ROI	Locus of R	<i>T</i>	<i>p</i>	MNI coordinates
PreDCA	Right postPU	4.41	0.02	[30, 3, -3]
PreDCA	Left preDCA	3.49	0.05	[-9, 12, 3]
PostCA	Right postPU	3.6	0.05	[30, 3, -3]
PreDCA	Left preDCA	4.61	0.02	[-9, 15, 0]

Table 5 Correlations between fMRI and PET. Pearson product moment correlations between fMRI contrasts of primary interest for β (*=absolute, **=normalized) and fMRI blood oxygenation level (BOLD) and ΔBP_{ND} in ventral striatum (VST) and posterior caudate (postCA). There were no significant correlations between fMRI activation and DA release with this method

fMRI contrast	ΔBP_{ND} VST		ΔBP_{ND} postCA	
	<i>R</i>	<i>p</i>	<i>r</i>	<i>p</i>
A1 Win\$5 vs. Win/lose\$0 (beta)*	-0.86	0.76	0.001	1.00
A1 Win\$5 vs. Win/lose\$0 (beta)**	0.392	0.15	0.180	0.54
A1 Win\$5 vs. Win/lose\$0 (BOLD)	-0.234	0.40	0.098	0.74
A1 Lose\$5 vs. Win/lose\$0 (BOLD)	0.374	0.17	-0.345	0.23

did not evaluate a separate ROI mask for the NAcc. NAcc is included in VST, but to maximize reliability, our operational definition requires inclusion of ventral caudate and putamen rostral to the anterior commissure. Voltammetry studies in rodents show the greatest activity in the NAcc during appetitive (anticipatory) rather than consummatory phases of reward (Richardson and Gratton 1996; Garris et al. 1999). We chose to model anticipatory and consummatory trials separately, and this might help explain why we found greater activation for the A1 phase rather than OC.

In our model, it also appeared that “prospect of reward” (A1) provided a stronger incentive than “anticipation of reward” (A2), maybe partially explained by the subjects' ability to predict fairly reliably whether they had responded correctly. These coordinates were located in the VST when the stimulus appeared, and thus were better able to predict the following feedback (“outcome”). As A2 thus represented less of a novelty, waiting for a more predictable outcome may have been less salient and activation may be little different from the consummatory phase itself.

Activation of the mesial prefrontal cortex/anterior cingulate by both rewards and punishments has also been demonstrated by Schott et al. (2008) and in more detail by Fujiwara et al. (2009). Similar to Schott et al., we found slightly more activation in left striatal areas both in fMRI group maps as well as a trend in the PET outcome measure.

PET

We did not detect a significant effect of MIDT performance on VST ΔBP_{ND} . We did, however, detect a significant difference in ΔBP_{ND} in the posterior caudate suggesting DA release in response to reward. This ROI, drawn as previously described (Martinez et al. 2003), comprises the dorsal part of the caudate, which has been linked to reward/punishment processing (Schultz et al. 2000). The signal in this region may have been augmented to a detectable level

by the motor component of the task, as simple motor tasks like finger tapping have been found to displace [^{11}C] raclopride in caudate and putamen in healthy subjects (Ouchi et al. 2002; Goerendt et al. 2003), albeit to a lesser degree than tasks involving both motor and cognitive components (Koepp et al. 1998; Lappin et al. 2009). Decreases in [^{11}C]raclopride binding have also been observed during several behavioral paradigms including playing an engaging video game (Koepp et al. 1998) as well as during exposure to (conditioned) sensory stimuli such as highly palatable food (Small et al. 2003), exposure to drug cues in drug addicts (Volkow et al. 2006), and during placebo administration of analgesics (Scott et al. 2007) and psychostimulants (Boileau et al. 2007).

Koepp et al. found a [^{11}C]raclopride displacement of -13% in the VST during a video game task, which is comparable to [^{11}C]raclopride displacement after pharmacological challenges with e.g., amphetamine (Koepp et al. 1998). An even larger effect of cognitive and reward-predicting components was suggested by Boileau et al. in subjects scanned with [^{11}C]raclopride after amphetamine or placebo. In that study, placebo decreased [^{11}C]raclopride binding in the VST to the same extent as amphetamine (23%) (Boileau et al. 2007). Also, a study in which Parkinson's disease patients were presented with different probabilities of receiving levodopa, while in fact receiving placebo, found a significant effect of expectation on [^{11}C]raclopride displacement in the VST and putamen (Lidstone et al. 2010). These findings suggest that conditioned cues associated with reward alone can increase DA transmission in striatal areas providing further evidence that this system is involved in reward prediction in humans. Other reports examining responses to monetary rewards have shown mixed results. In a study in which response to a gambling task (simulated slot machine) led to monetary rewards on an unpredictable subset of trials, Martin-Soelch et al. (2011) observed modest decreases in [^{11}C]raclopride binding in the VST (the overall decrease in VST was approximately 4%) that had some dependency on sex and laterality (neither effect of sex nor effect of laterality nor their interaction were statistically significant in VST in the current study nor were significant effects of sex or sex by laterality interaction observed in any ROI, data not shown). Hakyemez et al. did not observe decreases in [^{11}C]raclopride binding in rewarded compared to unrewarded trials using a design in which monetary rewards were given on an unpredictable subset of passively viewed trial presentations, and in fact, saw increased binding in the dorsal putamen suggestive of reduced DA transmission (Hakyemez et al. 2008).

Unlike Schott et al. (2008) who published the first study to directly investigate the relationship between reward-related striatal DA release and the fMRI correlates

of reward anticipation and found significant [^{11}C]raclopride displacement in the left VST during the rewarded condition, and despite a similar design, we did not observe measureable change in [^{11}C]raclopride binding across conditions. In Schott et al.'s (2008) experiment, PET sessions were carried out on two different days. One day contained a majority of neutral trials (135 neutral:45 rewarded), the other day had the reversed ratio of rewarded and unrewarded conditions (135 rewarded:45 nonrewarded), and a mean hit (win) rate of 80%. In our study, the “neutral” condition was a simple baseline scan with no task performance and the “rewarded” condition provided an adjusted win:negative outcome ratio of 64:36 to make the task more salient by keeping a favorable win ratio. If rewarding stimuli induce DA release and decrease [^{11}C]raclopride binding, while “nonreward” may actually reduce DA levels, the combination of rewarding and nonrewarding stimuli during a single scan may have led to an overall weakening of the effect on DA release, despite the overall bias to win. The difference between the two results may be related to a slightly more favorable win ratio in the design of Schott vs. ours. Timing relative to the PET scan may have also decreased the likelihood of detecting changes in BP_{ND} : in our design, MIDT was carried out while equilibrium between [^{11}C]raclopride concentration in blood plasma, striatum and cerebellum was being established but ended before the emission scan began—small changes in DA release induced by the task may have been too transient to cause detectable changes in [^{11}C] raclopride binding. We adopted this design to minimize the effects of task performance on head motion during the scanning session that would result in motion-related decrease in the signal.

Correlational analysis

Pharmacological fMRI (Pessiglione et al. 2006) and correlations between [^{11}C]raclopride $\Delta\text{BP}_{\text{ND}}$ and reward activation of the VST (Schott et al. 2007) have suggested a quantitative role for DA signaling in the ventral striatal reward anticipation response in humans. Schott et al. demonstrated that under constant task conditions, the VST hemodynamic response to reward anticipation correlates positively with DA release in the same rewarded task. We failed to detect a relationship between the two imaging modalities' outcome measures in the ROI-based analysis of correlations between $\Delta\text{BP}_{\text{ND}}$ and subjects' β coefficients in the corresponding ROI, possibly due to the lack of observable [^{11}C]raclopride displacement. We would have predicted that using $\Delta\text{BP}_{\text{ND}}$ from an ROI as a covariate, voxelwise correlations with fMRI contrasts would be localized to the same ROI as the covariate. This was the case for the preDCA, but the fact that ROIs were not

entirely congruent may also suggest the possibility that fMRI activation is not entirely explained by DA release.

Our results here again differ from Schott who found a positive correlation between neural activity of the SNC/VTA during reward anticipation and reward-related [^{11}C] raclopride displacement in the VST (Schott et al. 2008). In that paper, the correlational analysis approach to the VST used selected “individual spherical ROIs” seeded at the individual local maxima identified by voxelwise analysis of PET data, while our analysis used a predefined anatomically driven ROI analysis. These differences in analytical approach may explain the difference in findings and suggest that the relationship, if present, may be at best attributed to few voxels rather than a global regional effect.

In conclusion, our study indicates that endogenous DA release may either be very modest or very difficult to detect with PET under conditions of a behavioral task where rewarding conditions are interspersed with nonrewarding conditions despite overall bias for winning. An alternative explanation may be that BOLD signal reflects changes in neuronal activity related to changes in excitatory tone, mostly driven by glutamate neurotransmission (Shulman et al. 2002). To our knowledge, this is only the second study to date that explores the relationship between functional and neurochemical imaging outcome measures using a monetary reward paradigm, and while some congruency in the findings between this and previous studies provides encouraging evidence for understanding the neurochemical changes underlying fMRI activity, further studies are needed.

Acknowledgements We would like to thank Mr. Ben Gunter for technical support with the fMRI arm of the study. This research was carried out at New York State Psychiatric Institute/Columbia University Medical Center under a subcontract from the Center for Translational Neuroscience of Alcoholism at Yale University, supported by grant number P50AA-012870-09 from the National Institute on Alcohol Abuse and Alcoholism. The funding agency had no role in the design and conduct of the study; in the collection, analysis, and interpretation of the data; or in the preparation, review, or approval of the manuscript.

Financial disclosures: M. Slifstein: consultant: Amgen, GlaxoSmithKline; research support: Pierre Fabre, Inc.; J.H. Krystal reports the following: consultant: Aisling Capital, LLC, AstraZeneca Pharmaceuticals, Brintnall & Nicolini, Inc., Easton Associates, Gilead Sciences, Inc., GlaxoSmithKline, Janssen Pharmaceuticals, Lundbeck Research USA, Medivation, Inc., Merz Pharmaceuticals, MK Medical Communications, F. Hoffmann-La Roche Ltd., SK Holdings Co., Ltd., Takeda Industries, Teva Pharmaceutical Industries, Ltd.; scientific advisory board: Abbott Laboratories, Bristol-Myers Squibb, Eisai, Inc., Eli Lilly and Co., Lohocla Research Corporation, Naurex, Inc., Pfizer Pharmaceuticals Exercisable Warrant Options (value less than \$500); Tetrigenex Pharmaceuticals; research/study drug support: Janssen Research Foundation (to the Department of Veterans Affairs); Board of Directors: Coalition for Translational Research in Alcohol and Substance Use Disorders, American College of Neuropsychopharmacology (President elect); Editor: Biological Psychiatry; inventions: 1) Seibyl JP, Krystal JH, Charney DS. Dopamine and

noradrenergic reuptake inhibitors in treatment of schizophrenia. Patent #: 5,447,948. September 5, 1995; 2) coinventor with Dr. Gerard Sanacora on a filed patent application by Yale University related to targeting the glutamatergic system for the treatment of neuropsychiatric disorders (PCTWO06108055A1); and 3) Intranasal Administration of Ketamine to Treat Depression (pending). A. Abi-Dargham: Bristol-Myers Squibb-Otsuka (consultant and speaker), Boehringer-Engelheim, Lundbeck, Sepracor, Merck (consultant), GlaxoSmithKline (research grant). All other authors reported no biomedical financial interests or potential conflicts of interest.

References

- Aarts E, Roelofs A et al (2010) Striatal dopamine mediates the interface between motivational and cognitive control in humans: evidence from genetic imaging. *Neuropsychopharmacology* 35 (9):1943–1951
- Andrews MM, Meda SA, et al. (2010). Individuals family history positive for alcoholism show functional magnetic resonance imaging differences in reward sensitivity that are related to impulsivity factors. *Biol Psychiatry*(Nov 30.): [Epub ahead of print].
- Arias-Carrion O, Poppel E (2007) Dopamine, learning, and reward-seeking behavior. *Acta Neurobiol Exp (Wars)* 67(4):481–488
- Ashburner J (2009) Computational anatomy with the SPM software. *Magn Reson Imaging* 27(8):1163–1174
- Bayer HM, Glimcher PW (2005) Midbrain dopamine neurons encode a quantitative reward prediction error signal. *Neuron* 47(1):129–141
- Boileau I, Dagher A et al (2007) Conditioned dopamine release in humans: a positron emission tomography [¹¹C]raclopride study with amphetamine. *J Neurosci* 27(15):3998–4003
- Cools R, Frank MJ et al (2009) Striatal dopamine predicts outcome-specific reversal learning and its sensitivity to dopaminergic drug administration. *J Neurosci* 29(5):1538–1543
- D'Ardenne K, McClure SM et al (2008) BOLD responses reflecting dopaminergic signals in the human ventral tegmental area. *Science* 319(5867):1264–1267
- First MB, Spitzer RL et al (1995) Structured clinical interview for DSM-IV axis I disorders. Biometrics Research, New York State Psychiatric Institute, New York
- Fujiwara J, Tobler PN et al (2009) Segregated and integrated coding of reward and punishment in the cingulate cortex. *J Neurophysiol* 6(101):3284–3293
- Garris PA, Kilpatrick M et al (1999) Dissociation of dopamine release in the nucleus accumbens from intracranial self-stimulation. *Nature* 398:67–69
- Goerendt IK, Messa C et al (2003) Dopamine release during sequential finger movements in health and Parkinson's disease: a PET study. *Brain* 126(Pt 2):312–325
- Haber SN, Fudge JL et al (2000) Striatonigrostriatal pathways in primates form an ascending spiral from the shell to the dorsolateral striatum. *J Neurosci* 20(6):2369–2382
- Hakymez HS, Dagher A et al (2008) Striatal dopamine transmission in healthy humans during a passive monetary reward task. *NeuroImage* 39(4):2058–2065
- Hall H, Sedvall G et al (1994) Distribution of D1- and D2-dopamine receptors, and dopamine and its metabolites in the human brain. *Neuropsychopharmacology* 11(4):245–256
- Knutson B, Westdorp A et al (2000) fMRI visualization of brain activity during a monetary incentive delay task. *NeuroImage* 12 (1):20–27
- Knutson B, Adams CM et al (2001a) Anticipation of increasing monetary reward selectively recruits nucleus accumbens. *J Neurosci* 21(16):RC159
- Knutson B, Fong GW et al (2001b) Dissociation of reward anticipation and outcome with event-related fMRI. *Neuroreport* 12(17):3683–3687
- Knutson B, Taylor J et al (2005) Distributed neural representation of expected value. *J Neurosci* 25(19):4806–4812
- Koepp MJ, Gunn RN et al (1998) Evidence for striatal dopamine release during a video game. *Nature* 393(6682):266–268
- Lappin JM, Reeves SJ et al (2009) Dopamine release in the human striatum: motor and cognitive tasks revisited. *J Cereb Blood Flow Metab* 29(3):554–564
- Laruelle M (2000) Imaging synaptic neurotransmission with in vivo binding competition techniques: a critical review. *J Cereb Blood Flow Metab* 20(3):423–451
- Laruelle M, Abi-Dargham A et al (1994) SPECT quantification of [¹²³I]iomazenil binding to benzodiazepine receptors in nonhuman primates: II. Equilibrium analysis of constant infusion experiments and correlation with in vitro parameters. *J Cereb Blood Flow Metab* 14(3):453–465
- Lidstone SC, Schulzer M et al (2010) Effects of expectation on placebo-induced dopamine release in Parkinson disease. *Arch Gen Psychiatry* 67(8):857–865
- Martinez D, Slifstein M et al (2003) Imaging human mesolimbic dopamine transmission with positron emission tomography. Part II: amphetamine-induced dopamine release in the functional subdivisions of the striatum. *J Cereb Blood Flow Metab* 23 (3):285–300
- Martinez D, Gil R et al (2005) Alcohol dependence is associated with blunted dopamine transmission in the ventral striatum. *Biol Psychiatry* 58(10):779–786
- Martin-Soelch C, Szczepanik J et al (2011) Lateralization and gender differences in the dopaminergic response to unpredictable reward in the human ventral striatum. *Eur J Neurosci* 33(9):1706–1715
- Mawlawi O, Martinez D et al (2001) Imaging human mesolimbic dopamine transmission with positron emission tomography: I. Accuracy and precision of D(2) receptor parameter measurements in ventral striatum. *J Cereb Blood Flow Metab* 21 (9):1034–1057
- Ouchi Y, Yoshikawa E et al (2002) Effect of simple motor performance on regional dopamine release in the striatum in Parkinson disease patients and healthy subjects: a positron emission tomography study. *J Cereb Blood Flow Metab* 22(6):746–752
- Pessiglione M, Seymour B et al (2006) Dopamine-dependent prediction errors underpin reward-seeking behaviour in humans. *Nature* 442(7106):1042–1045
- Rademacher L, Krach S et al (2010) Dissociation of neural networks for anticipation and consumption of monetary and social rewards. *NeuroImage* 49(4):3276–3285
- Richardson NR, Gratton A (1996) Behavior-relevant changes in nucleus accumbens dopamine transmission elicited by food reinforcement: an electrochemical study in rat. *J Neurosci* 16:8160–8169
- Schott BH, Niehaus L et al (2007) Ageing and early-stage Parkinson's disease affect separable neural mechanisms of mesolimbic reward processing. *Brain* 130(Pt 9):2412–2424
- Schott BH, Minuzzi L et al (2008) Mesolimbic functional magnetic resonance imaging activations during reward anticipation correlate with reward-related ventral striatal dopamine release. *J Neurosci* 28(52):14311–14319
- Schultz W (1998) Predictive reward signal of dopamine neurons. *J Neurophysiol* 80(1):1–27
- Schultz W, Apicella P et al (1992) Neuronal activity in monkey ventral striatum related to the expectation of reward. *J Neurosci* 12(12):4595–4610
- Schultz W, Dayan P et al (1997) A neural substrate of prediction and reward. *Science* 275:1593–1599

- Schultz W, Tremblay L et al (2000) Reward processing in primate orbitofrontal cortex and basal ganglia. *Cereb Cortex* 10(3):272–284
- Scott DJ, Stohler CS et al (2007) Individual differences in reward responding explain placebo-induced expectations and effects. *Neuron* 55(2):325–336
- Shulman RG, Hyder F, Rothman DL (2002) Biophysical basis of brain activity: implications for neuroimaging. *Q Rev Biophys* 35(3):287–325
- Small DM, Jones-Gotman M et al (2003) Feeding-induced dopamine release in dorsal striatum correlates with meal pleasantness ratings in healthy human volunteers. *NeuroImage* 19(4):1709–1715
- Sutton, R. S. and A. G. Barto (1998). Reinforcement learning: an introduction adaptive computation and machine learning, The MIT Press. 3.
- Volkow ND, Wang GJ et al (2006) Cocaine cues and dopamine in dorsal striatum: mechanism of craving in cocaine addiction. *J Neurosci* 26(24):6583–6588
- Zald DH, Boileau I et al (2004) Dopamine transmission in the human striatum during monetary reward tasks. *J Neurosci* 24(17):4105–4112